PHYSICAL REVIEW B **80**, 060401(R) (2009)

# Excitation of two spatially separated Bose-Einstein condensates of magnons

O. Dzyapko,[1] V. E. Demidov,[1] M. Buchmeier,[1] T. Stockhoff,[2] G. Schmitz,[2] G. A. Melkov,[3] and S. O. Demokritov[1,*]
[1]*Institute for Applied Physics, University of Münster, 48149 Münster, Germany*
[2]*Institute of Material Physics, University of Münster, 48149 Münster, Germany*
[3]*Department of Radiophysics, National Taras Schevchenko University of Kiev, Kiev 01033, Ukraine*
(Received 19 June 2009; published 14 August 2009)

We have studied experimentally the spatial properties and the dynamics of magnon Bose-Einstein condensates created in ferromagnetic films by a parametric pumping with different spatial configurations. Using the specific character of dynamic fields produced by pumping resonators of different shapes, we were able to realize the regime, in which two spatially separated condensates of magnons are formed. Our experiments show that while the separation between the condensates is determined by the size of the resonator, their spatial width can be changed by varying the power of the pumping signal.

DOI: 10.1103/PhysRevB.80.060401 PACS number(s): 75.45.+j, 75.40.Gb, 03.75.Nt

After the experimental observation of Bose-Einstein condensation (BEC) of atoms[1] and different quasiparticles[2,3] numerous investigations on manipulation of single condensates and interaction of two or more condensates have been carried out. In the case of atomic gases the experiments on the interference of two condensate clouds allowed the investigation of the coherence properties of condensates.[4] Furthermore, coherent interaction of condensates gives rise to a large variety of interesting basic effects. In particular, Josephson oscillations were observed in the system of two weakly interacting condensates of dilute gases.[5,6] It was also shown that, due to the strongly nonlinear character of the interaction between atomic condensates, the effect of nonlinear self-trapping can appear.[6]

Systems of quasiparticles enabling easy control of particle densities through external pumping mechanisms are very promising candidates for observation and investigation of the above phenomena. Nevertheless, despite numerous theoretical predictions of these effects for condensates of excitons and polaritons (see, e.g., Refs. 7 and 8), no experimental results have been reported yet. Along with excitons and polaritons, an observation of BEC in a parametrically driven gas of magnons was recently reported.[9] It was shown that exciting a magnon gas by a microwave field, one can achieve the critical density necessary for the Bose-Einstein transition and observe the formation of the condensate at room temperature. Recently a number of detailed experimental studies of BEC of magnons with temporal and frequency resolution, as well as with the resolution with respect to their wave vectors were reported,[10–12] followed by numerous theoretical works.[13–17] These investigations have proven the concept of magnon BEC under the influence of microwave parametric pumping and demonstrated the large potential of the magnon system for general studies of the BEC phenomena. Nevertheless, the spatial properties of magnon condensates and their spatiotemporal dynamics remain not sufficiently addressed.

Here we report on the spatially resolved experimental investigation of Bose-Einstein condensates of magnons driven by a microwave pumping field of different spatial configurations. Using the sensitivity of Brillouin light scattering (BLS) technique with respect to the frequency of magnons in combination with its high temporal and spatial resolution we were able to map the distributions of the condensate density and investigate its spatiotemporal dynamics. For a particular geometry of the pumping resonator we observed a simultaneous excitation of two spatially separated magnon condensates. Our findings open a way for further experiments on the study of condensate interactions. They show that the spatial characteristics of the condensates can be easily controlled by the geometry of the resonator and the power of the pumping signal.

A sketch of the experimental setup is shown in Fig. 1(a). We used a 5.1-$\mu$m-thick monocrystalline yttrium iron garnet (YIG) film epitaxially grown on a transparent gadolinium garnet substrate (not shown in Fig. 1 for clarity). The sample with lateral dimensions of $2\times 10$ mm was placed into a uniform static magnetic field $H_0=1000$ Oe applied in its plane parallel to the long side. The excitation of magnons was performed by means of microwave parametric pumping. For this a half-wavelength microwave resonator was placed close to the sample surface perpendicularly to the long side of the sample. A microwave pumping signal with peak power $P$ in

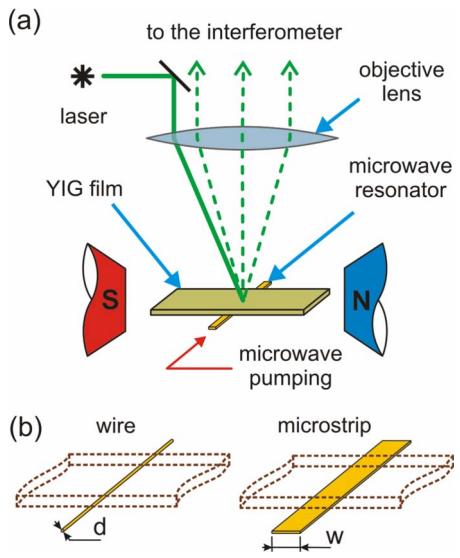


FIG. 1. (Color online) (a) Schematics of the experimental setup. (b) Layout of the microwave resonators used in the experiment.

 

the range from 1 to 8 W was applied to the resonator. To avoid thermal overheating of the sample by microwaves, the pumping was performed in a pulsed regime with a duration of microwave pulses of 1 $\mu$s and a repetition frequency of 50 kHz. In order to examine the influence of the shape of the pumping resonator on the spatial properties of the condensate, measurements with two different types of resonators were performed, as sketched in Fig. 1(b). The resonators of the first type were wires with a diameter $d=25$ $\mu$m, similar to those used in the previous experiments on the magnon BEC.[9–12] The resonators of the second type were stripes with a width $w=500$ $\mu$m and a thickness of 10 $\mu$m made from a 50 Ohm microstrip transmission line. The resonators of both types were tuned to have the same resonant frequency $f_p \approx 8.1$ GHz.

The spatial distribution of the condensate created in the YIG film was probed by means of BLS spectroscopy in quasibackward scattering geometry.[18] The probing beam produced by a single-frequency laser operating at $\lambda=532$ nm was focused by a wide-angle objective lens with a numerical aperture of 0.42 onto the surface of the YIG film, as shown in Fig. 1(a). By analyzing the spectrum of the light inelastically scattered from magnons in the YIG film, we determined the distributions of magnons over frequencies and their temporal evolution.[9] The spatial resolution was realized by a movement of the sample with respect to the focal spot and reached down to 10 $\mu$m, being limited mainly by the size of the spot. Note that the pumping resonator was displaced from the surface of the YIG film by 15–100 $\mu$m, depending on its dimensions, in order to reduce the influence of the light reflected from its surface on the obtained spatial maps of the BLS intensity.

In the first step, the formation of BEC was confirmed by the observation of an enormous overpopulation of the magnon state corresponding to the minimum frequency of the magnon spectrum $f_{\min}$, resulting in the appearance of a powerful narrow peak in the BLS spectra.[9] The frequency $f_{\min}$ was found to be equal to about 2.9 GHz for both used pumping geometries. Then we performed spatially resolved measurements of the intensity of the above peak, scanning the probing focal spot over the surface of the sample in the proximity of the resonator. In this way, two-dimensional maps of the BLS intensity, proportional to the density of the condensate, were obtained for different pumping powers and temporal delays $t$ with respect to the start of the pumping pulse. As one would expect from the symmetry reasons, the obtained maps were found to be uniform along the length of the resonators. Therefore, we will restrict the discussion below to the analysis of one-dimensional distributions of the condensate density over the spatial coordinate $z$ perpendicular to the axis of the resonator and their temporal dependences.

Figure 2 presents typical results of the spatially and temporally resolved measurements for the wire [Fig. 2(a)] and the microstrip [Fig. 2(b)] resonators at $P=4$ W. Figure 2 shows maps of the intensity of the BLS peak at $f_{\min}$ as a function of the transverse coordinate $z$ and the temporal delay $t$ ($t=0$ corresponds to the start of the pumping pulse). The spatial profiles of the BLS intensity corresponding to the end of the pumping pulse ($t=1$ $\mu$s) are shown as well.

First, let us consider the results obtained using the wire

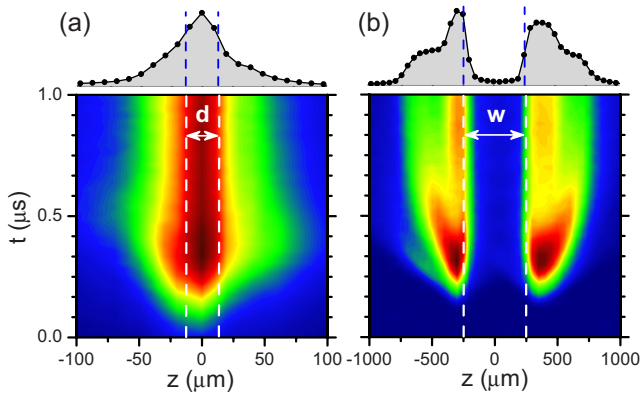


FIG. 2. (Color online) Color-coded representation of the BLS intensity at the frequency of the lowest magnon state portraying the density of the magnon condensate as a function of the spatial coordinate $z$ perpendicular to the axis of the resonator and the temporal delay with respect to the start of the pumping pulse $t$ for the case of the (a) wire and the (b) microstrip resonators. Close to the maps the spatial profiles of the BLS intensity are shown corresponding to the end of the pumping pulse ($t=1$ $\mu$s). Dashed lines show the geometrical boundaries of the pumping resonators. Pumping power $P=4$ W.

resonator [see Fig. 2(a)]. The graph shows that the formation of the condensate is slightly delayed with respect to the start of the pumping pulse, which is associated with the finite time needed for the thermalization of the magnon gas.[10] It is also seen in Fig. 2(a) that the condensate exhibits an initial spatial expansion, but then its width slightly decreases and the spatial distribution stabilizes. The later decrease is possibly due to the action of a weak attractive interaction between magnons,[14] and, as will be shown below, becomes more pronounced with increase in the pumping power. The main feature of the formed condensate cloud is that it is concentrated over the resonator and has a maximum over its center.

Completely different spatial distributions were observed as the wire resonator was replaced by a microstrip [see Fig. 2(b)]. Although all the parameters of the experiment were the same, the observed picture drastically differs from that shown in Fig. 2(a): instead of one condensate cloud concentrated over the resonator, two condensates are formed. The condensates appear to be well separated in space and the distance between them does not change with time. Mapping the position of the resonator onto the graph (dashed lines) one can clearly see that the condensates are located at the edges of the resonator so that the spatial separation between them is equal to the width of the microstrip $w$, whereas the density of the condensate over the center of the resonator is almost zero. Despite completely different spatial distributions, the temporal dynamics of the condensate clouds appear to be qualitatively similar to that in the case of the wire resonator: a slight initial expansion of the condensate is followed by its compression and a final stabilization.

Since the spatial distributions of the condensate density appear to be closely connected with the configuration of the pumping resonator, let us consider the process of the parametric pumping of magnons in detail. According to Suhl[19] and Schlömann[20] two different mechanisms of parametric

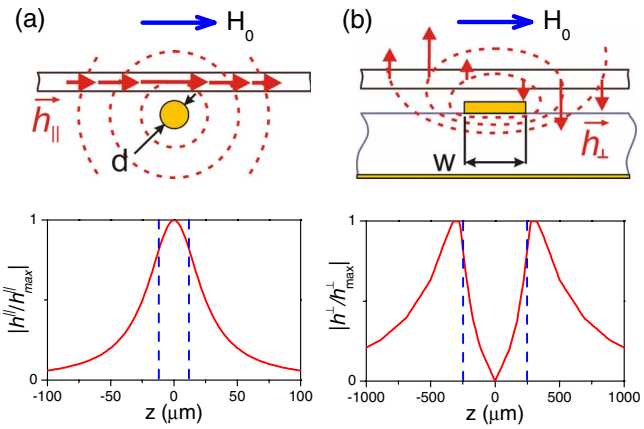


FIG. 3. (Color online) Schematic layout of the cross-section of the experimental structures and the spatial distributions of the dynamic magnetic fields produced by the (a) wire and the (b) microstrip pumping resonators.

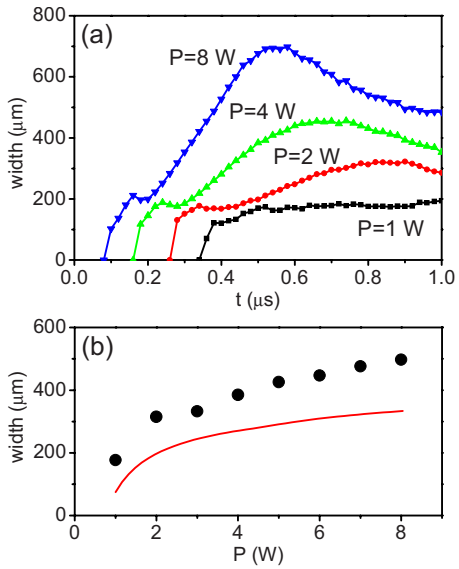


FIG. 4. (Color online) (a) Temporal dependences of the spatial width of the condensate clouds for the case of the two-condensate regime for different pumping powers $P$, as indicated. (b) Width of the condensate clouds corresponding to the end of the pumping pulse as a function of the pumping power. Points: experiment; line: theory.

instability of magnons exist. The first mechanism, named by Suhl as subsidiary absorption, is the instability of certain groups of magnons in a ferromagnet subjected to the dynamic magnetic field applied perpendicularly to the direction of the static magnetization. In the second case, called parallel pumping instability, magnons are excited by a dynamic magnetic field, which is parallel to the static magnetization. Since the pumping field created by the used resonators, has components both parallel and perpendicular to the static magnetization, both kinds of instabilities can occur in our experiments. Such a case of an oblique pumping was addressed in detail in Refs. 21 and 22. The main conclusion of these works is that under given experimental conditions the instability characterized by a smaller power threshold completely dominates over the other. Using the theory developed in Ref. 23, we calculated the threshold values of the dynamic magnetic field for the parallel and the perpendicular instabilities for our experimental conditions. They were found to be $h_{thr}^{\parallel} \approx 0.99$ Oe and $h_{thr}^{\perp} \approx 0.75$ Oe; i.e., they are rather close to each other.

Let us now analyze the structure of microwave magnetic fields produced by the wire and the microstrip resonators (see Fig. 3). The magnetic field of the wire resonator [Fig. 3(a)] can be calculated in the first approximation as $\vec{h}(r) = \frac{1}{2\pi}\frac{\vec{I}\times\vec{r}}{r^2}$. For this geometry the maximum of the parallel component of the field inside the YIG film is achieved above the center of the wire, while the maxima of the perpendicular component appear in two points separated from each other by the double distance from the wire axis to the film. However, the maximum values for the two components are essentially different: $h_{\max}^{\parallel} = 2h_{\max}^{\perp}$. Thus, the parallel pumping mechanism should strongly dominate for the case of the wire resonator. On the contrary, calculations of the components of the microwave field of the microstrip resonator[24] inside the film give $h_{\max}^{\parallel} \approx h_{\max}^{\perp}$. Taking into account that the threshold of the perpendicular pumping is smaller than that of the parallel one, the former should dominate for the case of the microstrip resonator. In accordance with these conclusions, the spatial distributions of the corresponding components of the dynamic magnetic field, shown in Fig. 3, appear to be very similar to the distributions of the condensate density presented in Fig. 2. This demonstrates that the variation in the geometry of the resonator allows one to switch between the two types of pumping and realize a simultaneous excitation of two magnon condensates separated by a distance defined by the width of the resonator.

As follows from the analysis of Fig. 2, the spatial width of the condensate clouds also depends strongly on the experimental conditions and, therefore, can be efficiently controlled. Figure 4(a) presents the temporal evolution of the width of the condensate clouds in the two-condensate regime for different pumping powers $P$. As discussed above, the curves in Fig. 4(a) show an initial expansion of the condensate clouds followed by a compression, which becomes more pronounced with the increase in $P$. The initial growth of the width can be associated with the process of formation of the condensate. Since the condensation is mediated by four-magnon scattering processes, which depend on the magnon density,[10] the condensate is first formed at the spatial point corresponding to the maximum of the pumping field, whereas its formation in the other spatial points takes more time. On the contrary, the subsequent decrease in the condensate width can be caused by the nonlinear dynamics of the already formed condensate.[14]

In spite of the presence of the above spatial dynamics, an important general conclusion about the increase in the width of the condensate cloud with increasing $P$ can be made from the analysis of Fig. 4(a). This tendency is further characterized by Fig. 4(b), where the experimentally determined width of the condensates at the end of the pumping pulse is shown as a function of $P$ by points. Such a dependence can be associated with the threshold character of the condensation process, which demands the density of magnons to be

larger than a certain critical value $n > n_{cr}$. It is obvious that with the increase in the pumping power the width of the spatial region, where the threshold of the condensation is reached increases as well. This width can be estimated based on the distribution of the pumping field, shown in Fig. 3(b), and the theory of the spatially homogeneous magnon condensation,[17] predicting that the density of magnons in the condensate is proportional to $\sqrt{h^2-h_{cr}^2}$, where $h$ is the microwave pumping field applied to the sample and $h_{cr}$ is its threshold value corresponding to the onset of BEC. The results of these calculations are shown in Fig. 4(b) by the line. Comparing the experimental and the theoretical data one can see their good qualitative agreement. Note that the experimentally determined width of the condensate appears to be slightly larger than the theoretical one. This result is expected since the spatially homogenous theory does not take into account an additional spreading of the condensate cloud due to the nonzero velocities of the magnons, existing at the intermediate stage between the pumping and the condensate. The same effect leads to the absence in Fig. 2 of an abrupt decrease in the condensate intensity at the spatial point, where the pumping field becomes smaller than the threshold field.

In conclusion, we have experimentally demonstrated that by simply varying the geometry of the pumping resonator one can efficiently control the spatial distributions of magnon condensates and realize the case, when two spatially separated condensate clouds are simultaneously created in a magnetic film. We show that the distance between the clouds and their spatial width can be varied in a controllable way. These findings create a base for further investigations of interaction between magnon condensates.

This work was supported in part by the Deutsche Forschungsgemeinschaft.

*Corresponding author; demokrit@uni-muenster.de

[1] C. Pethick and H. Smith, *Bose-Einstein Condensation in Dilute Gases* (Cambridge University Press, Cambridge, England, 2002).

[2] S. A. Moskalenko and D. W. Snoke, *Bose Einstein Condensation of Excitons and Biexcitons* (Cambridge University Press, Cambridge, England, 2000).

[3] J. Kasprzak, M. Richard, S. Kundermann, A. Baas, P. Jeambrun, J. M. J. Keeling, F. M. Marchetti, M. H. Szymanska, R. André, J. L. Staehli, V. Savona, P. B. Littlewood, B. Deveaud, and Le Si Dang, Nature (London) **443**, 409 (2006).

[4] M. R. Andrews, C. G. Townsend, H.-J. Miesner, D. S. Durfee, D. M. Kurn, and W. Ketterle, Science **275**, 637 (1997).

[5] F. S. Cataliotti, S. Burger, C. Fort, P. Maddaloni, F. Minardi, A. Trombettoni, A. Smerzi, and M. Inguscio, Science **293**, 843 (2001).

[6] M. Albiez, R. Gati, J. Fölling, S. Hunsmann, M. Cristiani, and M. K. Oberthaler, Phys. Rev. Lett. **95**, 010402 (2005).

[7] M. Wouters and I. Carusotto, Phys. Rev. Lett. **99**, 140402 (2007).

[8] I. A. Shelykh, D. D. Solnyshkov, G. Pavlovic, and G. Malpuech, Phys. Rev. B **78**, 041302(R) (2008).

[9] S. O. Demokritov, V. E. Demidov, O. Dzyapko, G. A. Melkov, A. A. Serga, B. Hillebrands, and A. N. Slavin, Nature (London) **443**, 430 (2006).

[10] V. E. Demidov, O. Dzyapko, S. O. Demokritov, G. A. Melkov, and A. N. Slavin, Phys. Rev. Lett. **99**, 037205 (2007).

[11] V. E. Demidov, O. Dzyapko, S. O. Demokritov, G. A. Melkov, and A. N. Slavin, Phys. Rev. Lett. **100**, 047205 (2008).

[12] V. E. Demidov, O. Dzyapko, M. Buchmeier, T. Stockhoff, G. Schmitz, G. A. Melkov, and S. O. Demokritov, Phys. Rev. Lett. **101**, 257201 (2008).

[13] A. I. Bugrij and V. M. Loktev, Low Temp. Phys. **33**, 37 (2007).

[14] I. S. Tupitsyn, P. C. E. Stamp, and A. L. Burin, Phys. Rev. Lett. **100**, 257202 (2008).

[15] V. M. Loktev, Low Temp. Phys. **34**, 178 (2008).

[16] S. M. Rezende, Phys. Rev. B **79**, 060410(R) (2009).

[17] S. M. Rezende, Phys. Rev. B **79**, 174411 (2009).

[18] S. O. Demokritov, B. Hillebrands, and A. N. Slavin, Phys. Rep. **348**, 441 (2001).

[19] H. Suhl, J. Phys. Chem. Solids **1**, 209 (1957).

[20] E. Schlömann, J. J. Green, and U. Milano, J. Appl. Phys. **31**, S386 (1960).

[21] Y. H. Liu and C. E. Patton, J. Appl. Phys. **53**, 5116 (1982).

[22] T. Neumann, A. A. Serga, V. I. Vasyuchka, and B. Hillebrands, Appl. Phys. Lett. **94**, 192502 (2009).

[23] O. G. Vendik, B. A. Kalinikos, and D. N. Chartorizhskii, Fiz. Tverd. Tela (Leningrad) **19**, 387 (1977) [Sov. Phys. Solid State **8**, 222 (1977)].

[24] A. Krawczyk and S. Wiak, *Electromagnetic Fields in Electrical Engineering* (IOS Press, 2002).